

Imaging the Spatial Density Within Starburst Galaxies M82 and Arp220



Nicholas S. Kern^{1,2}, Jeffrey G. Mangum², Jeremy K. Darling³, Christian Henkel⁴, Karl Menten⁴

¹University of Michigan, ²National Radio Astronomy Observatory, ³University of Colorado, ⁴Max-Planck-Institut für Radioastronomie



Purpose

In order to better understand starburst galaxies and the role they play in cosmic evolution, it is imperative to have a comprehensive understanding of their dense molecular gas regions and the physical conditions therein, which fuels the starburst activity. In this work, we present imaging of formaldehyde rotational transitions in the nuclei of starburst galaxies M82 and Arp220 using the Very Large Array, with the goal of deriving the physical conditions of extragalactic star forming regions. We map the formaldehyde (H_2CO) traced dense gas as a function of position and velocity across each galaxy. Using large velocity gradient models to simplify the radiative transfer, we also derive molecular hydrogen spatial densities (cm^{-3}) on resolution scales of ~ 7 arcseconds and 3.9 km/s. By using recently updated ammonia thermometry, we provide new measurements of the physical conditions of the dense gas in M82 and Arp220.

Dense Gas in M82

The molecular emission from M82 is found over a $40'' \times 15''$ disk-like structure in the nuclear region of the galaxy. In this work, we confirm H_2CO signatures from three distinct dense gas components in M82, which correspond to the South-West (SW) and North-East (NE) components found from other CO and high density tracers, as well as a Central (Cen) component between them. With a beam size of $\sim 7''$, we spatially resolve each component, and derive hydrogen spatial densities for each.

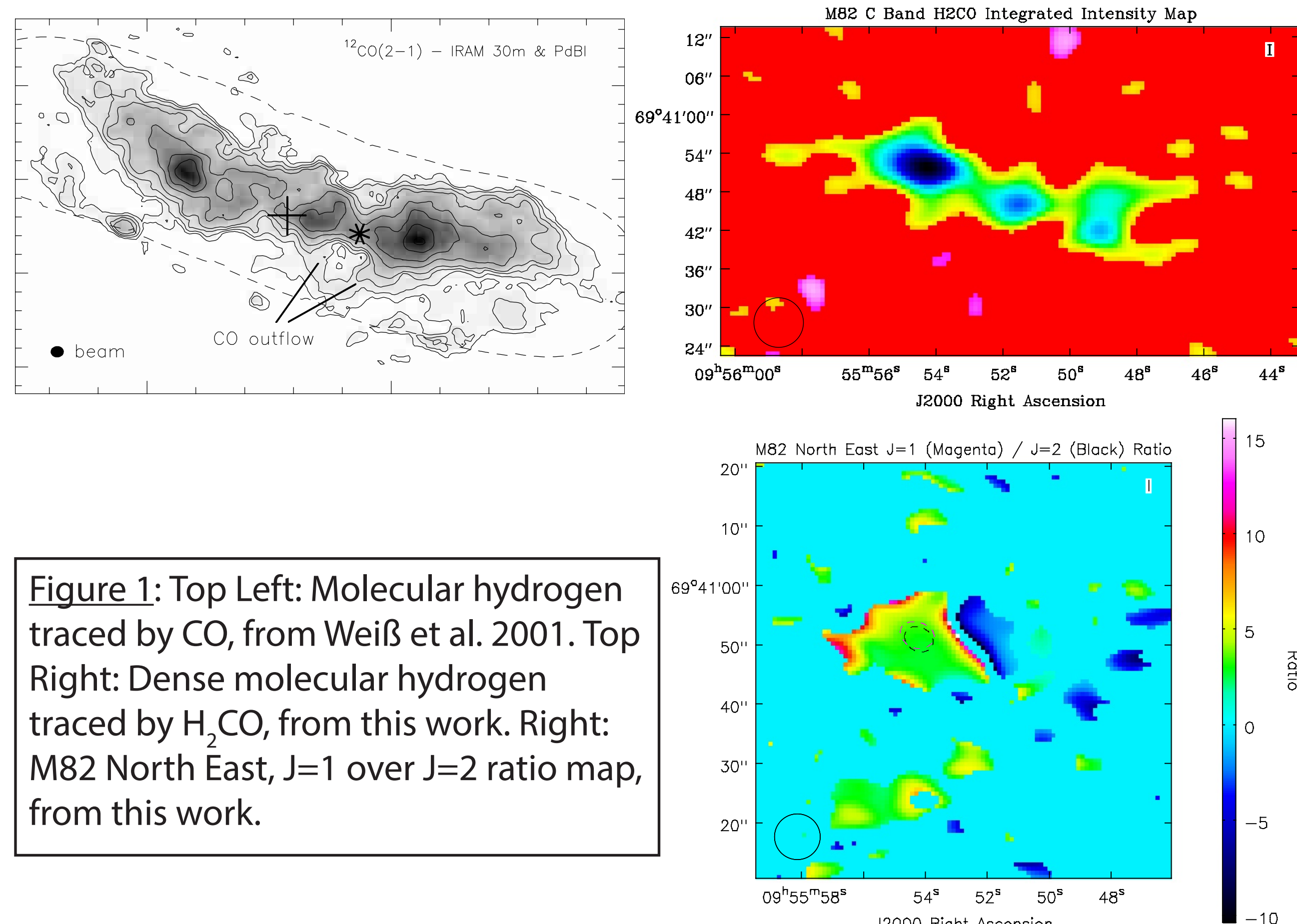


Figure 1: Top Left: Molecular hydrogen traced by CO, from Weiß et al. 2001. Top Right: Dense molecular hydrogen traced by H_2CO , from this work. Right: M82 North East, J=1 over J=2 ratio map, from this work.

We detect both the $1_{10}-1_{11}$ and $2_{11}-2_{12}$ transitions in absorption, which agrees with other H_2CO measurements and constrains $n(\text{H}_2) < 10^{5.5}$. NH_3 thermometry puts the kinetic temperature of M82SW at $\sim 50\text{K}$, and due to a lack of NH_3 detection in the Central and NE components, we assume the same fit. Using a 50K calibrated LVG model, we derive a $\log[n(\text{H}_2)]$ between 4.7 and 5.0. For reference, our beam of 7 arcseconds corresponds to a size of ~ 130 pc at M82's distance.

As a followup to Mangum et al. 2013a's study using the GBT, this research is motivated by the need to derive spatial densities of star forming regions at higher spatial resolutions. Measurements with the GBT derived $\log[n(\text{H}_2)] \sim 4.90 - 5.05$ with a $T_K \sim 50\text{K}$, which is a good fit to our results, however, using the VLA we are able to differentiate between the dense molecular lobes within M82's nuclear regions. Our results suggest that the NE component of M82 may hold some of the densest gas in the galaxy, and supports the notion that the dense molecular gas is located in circumnuclear lobes.

Other authors point out that because NH_3 is easily photodissociated, M82's low kinetic temperature fit probably traces a very dense and well shielded gas phase that only makes up a small portion of the total gas column density. In light of this, it is important to note that it is the dense gas phase of H_2 that will most likely contribute a large portion of the fuel for the next generation of star formation, which makes H_2CO traced dense gas with an NH_3 calibrated T_K a very informative measurement.

Dense Gas in Arp220

Arp220 is characterized as a late merger system with two nuclei embedded in a circumnuclear disk, called the Western (blueshifted) and Eastern (redshifted) nuclei. We cannot spatially resolve the nuclei, which are separated by only a few tenths of an arcsecond. We do spectrally resolve the double horn profile found in many other dense gas tracers (Greve et al. 2009), which is evidence of the two distinct nuclei. We find a v_{hel} of ~ 5325 km/s and ~ 5480 km/s, corresponding to the Western and Eastern nuclei respectively. Both have FWHM ranges of about 100-150 km/s and have a small velocity overlap within the line profile.

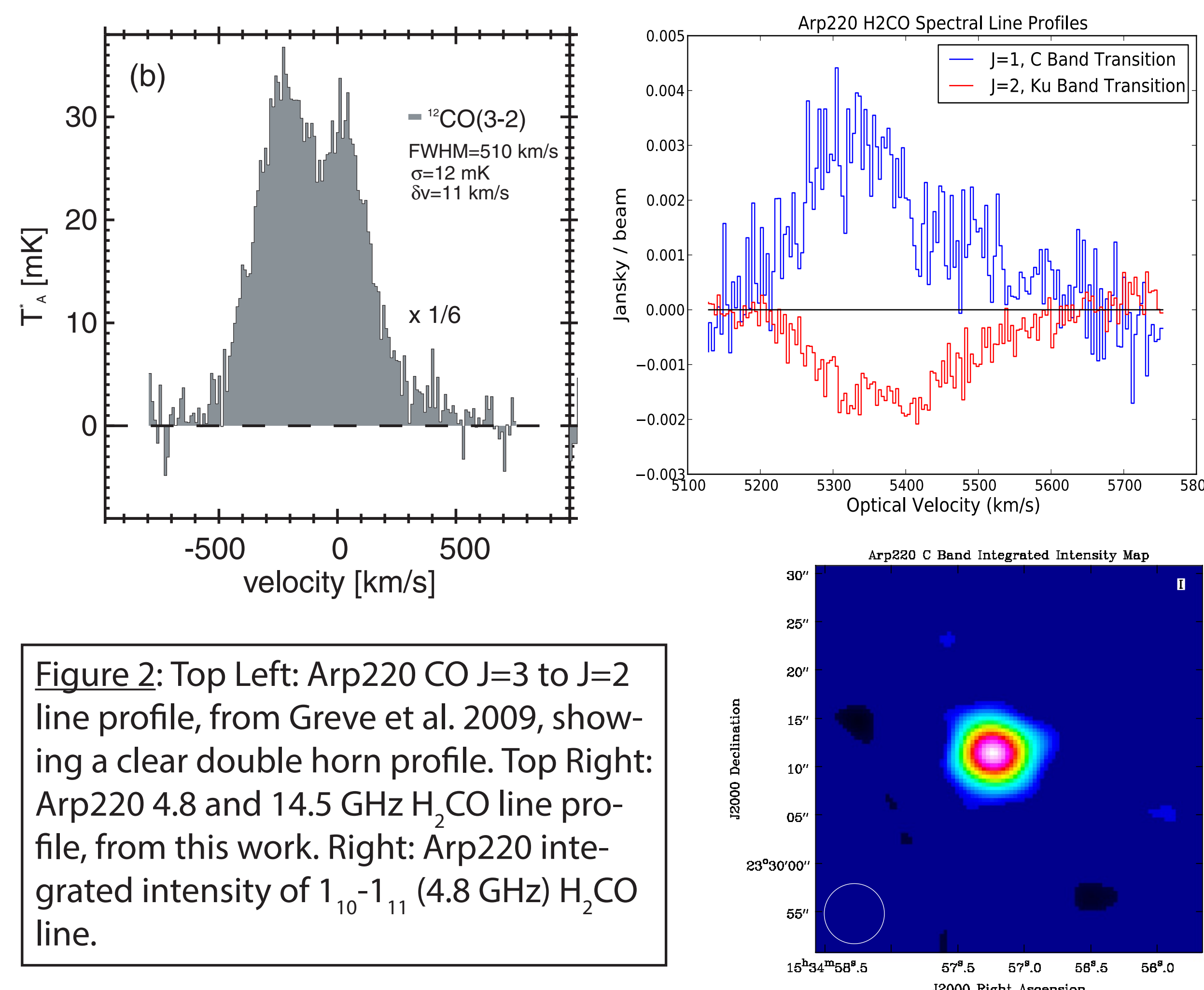


Figure 2: Top Left: Arp220 CO J=3 to J=2 line profile, from Greve et al. 2009, showing a clear double horn profile. Top Right: Arp220 4.8 and 14.5 GHz H_2CO line profile, from this work. Right: Arp220 integrated intensity of $1_{10}-1_{11}$ (4.8 GHz) H_2CO line.

We detect the $1_{10}-1_{11}$ transition in emission and the $2_{11}-2_{12}$ transition in absorption. Mangum et al. 2013a showed that the physical conditions necessary to create $1_{10}-1_{11}$ emission requires very high spatial densities, and because we detect strong emission, we can conclude that H_2CO is tracing some of the densest gas found in Arp220. We integrate both velocity structures and derive spatial densities for both nuclei, but because there is some velocity overlap our results are likely to be somewhat biased. NH_3 thermometry describes similar kinetic temperatures in both nuclei, which alleviates this issue, but the next clear step in understanding the unique H_2CO emission in Arp220 is to follow up these observations with high spatial resolution measurements, so as to completely distinguish the two nuclei.

Additionally, the fact that the 14.5 GHz transition is subsequently found in absorption constrains the H_2CO traced dense gas in Arp220 to a narrow range of densities. For an LVG model with kinetic temperatures ranging from T_K from 50K - 250K, $\log[n(\text{H}_2)]$ ranges from 4.5 - 5.5. Ammonia thermometry from Mangum et al. 2013b describe a two temperature fit for both nuclei at $\sim 150\text{K}$ and $\sim 200\text{K}$. For both nuclei we derive $\log[n(\text{H}_2)] = 5.2 \pm 0.1$ and 4.9 ± 0.2 , for T_K of 150K and 200K respectively.

Formaldehyde Densitometry

The excitation of the $1_{10}-1_{11}$ and $2_{11}-2_{12}$ rotational transitions of formaldehyde at 4.8 and 14.5 GHz, respectively, are governed by spatial density and kinetic temperature. These "K-doublet" transitions have a unique sensitivity to spatial density, which allows them to be collisionally cooled when $n(\text{H}_2) < 10^{5.5}$, thus allowing them to appear in absorption against the cosmic microwave background. Using a simplified model of the radiative transfer and an assumed kinetic temperature of the region, one can derive a spatial density of molecular hydrogen, $n(\text{H}_2) \text{ cm}^{-3}$.

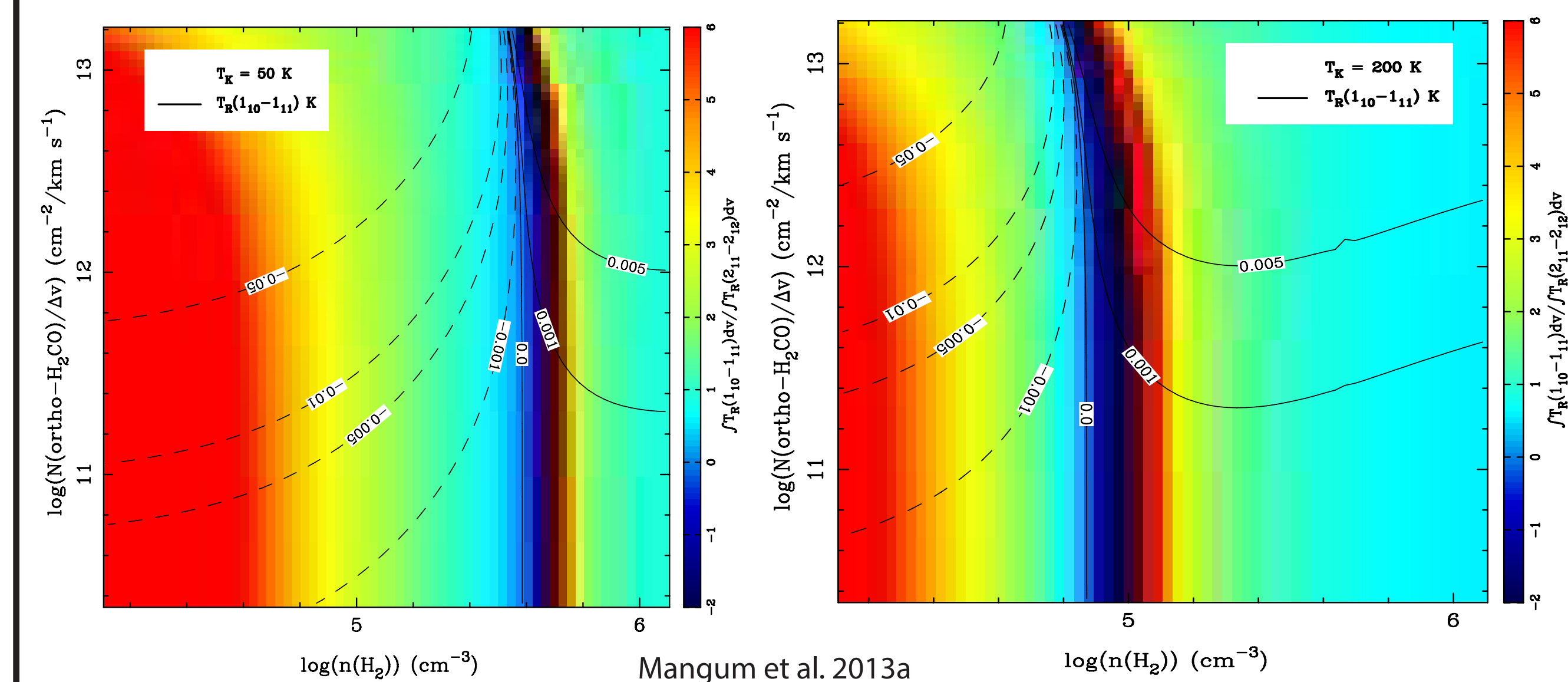


Figure 3: Large velocity gradient models for kinetic temperatures of 50 K (left) and 200 K (right). The x-axis is the logarithm of molecular hydrogen spatial density. The colors represent the ratio of the $1_{10}-1_{11}$ over the $2_{11}-2_{12}$ transition integrated intensity. Previous measurements of the H_2CO column density restrict us to the lower half of each graph (Mangum et al. 2013a). LVG models are dependent on collisional excitation rates for a given molecule. For H_2CO , these are known to $\sim 20\%$, which implies an additional 20% error bar to our $n(\text{H}_2)$ calculations.

Derived Quantities

Dense Gas Component	$T_{\text{Kinetic}} (\text{K})^a$	J=1 / J=2 Ratio	$\log[n(\text{H}_2)] (\text{cm}^{-3})$
Arp220 Western Nucleus	150 / 200 \pm 30	-1.89 - -1.47	5.2 \pm 0.1 / 4.9 \pm 0.2
Arp220 Eastern Nucleus	150 / 200 \pm 30	-1.35 - -0.91	5.2 \pm 0.1 / 4.9 \pm 0.2
M82 South West	50 \pm 20	3.3 - 4.3	4.8 \pm 0.1
M82 Central	50 \pm 20	2.9 - 6.8	4.75 \pm 0.25
M82 North East	50 \pm 20	2.7 - 3.7	4.9 \pm 0.1

Notes: ^aKinetic Temperatures taken from Mangum et al. 2013b. Note Arp220 has a two temperature fit, $\sim 150\text{K}$ and $\sim 200\text{K}$, outlined in the same paper

Galaxy	4.8 GHz			14.5 GHz		
	EVLA (Jy)	GBT (Jy)	NED (Jy)	EVLA (Jy)	GBT (Jy)	NED (Jy)
M82	2.782	3.233	3.67–3.96	1.157	1.304	1.73
Arp220	0.203	0.217	0.22	0.097	0.082	0.11

Notes: NED values taken from Mangum et al. 2013a

Table 1: Derived transition ratios and molecular hydrogen spatial densities
Table 2: VLA continuum measurements from this work, GBT and NED measurements taken from Mangum et al. 2013a

Acknowledgements and References

This research was supported by the National Science Foundation's REU grant. I would like to thank all of the NRAO faculty and staff for a great REU experience, and especially Jeff Mangum for being a helpful and encouraging advisor.

Greve, T. R. et al. 2009, ApJ, 692, 1432
 Mangum, J. G. et al. 2013a, ApJ, 766, 108
 Mangum, J. G. et al. 2013b, ApJ, 779, 1411
 Weiß, A. et al. 2001, A&A, 365, 571

